ISSN 1064-2269, Journal of Communications Technology and Electronics, 2018, Vol. 63, No. 8, pp. 841–849. © Pleiades Publishing, Inc., 2018.
Original Russian Text © Yu.N. Kazantsev, G.A. Kraftmakher, V.P. Mal'tsev, V.S. Solosin, 2018, published in Radiotekhnika i Elektronika, 2018, Vol. 63, No. 8, pp. 765–774.

ELECTRODYNAMICS AND WAVE PROPAGATION

Periodic Arrays of Magnetoelectrically Excited Double and Single Split-Ring Resonators as Artificial Magnetic Conductors

Yu. N. Kazantsev[a], *, G. A. Kraftmakher[a], V. P. Mal'tsev[a], and V. S. Solosin[a]

[a] *Kotel'nikov Institute of Radio Engineering and Electronics, Russian Academy of Sciences (Fryazino Branch), Fryazino, Moscow oblast, 141190 Russia*

**e-mail: yukazantsev@mail.ru*

Received March 31, 2017

Abstract—The amplitude and phase of the reflection coefficient of periodic arrays of electrically conducting elements in the form of double and single split rings are determined for two orientations of these rings, corresponding to magnetic (*H*) and magnetoelectric (*HE*) excitation. It is shown that, in the case of the *HE*-excitation of the rings, the arrays possess the properties of an artificial magnetic conductor or a high-impedance surface. The electric and magnetic fields near the arrays are calculated, and the dependence of the impedance on the distance between the array and the plane in which the impedance is determined is obtained. It is shown that the maximum of the impedance is in close vicinity of the array and can amount to tens of thousands of ohms. The feasibility of implementing a modified Salisbury radio absorber of small thickness by means of such arrays is shown theoretically and experimentally. It is also shown that, under illumination of an array of limited dimensions by a closely placed dipole, the screening effect reaches −30 dB with good matching of the dipole to the feed line (the reflection coefficient in the line is less than −20 dB).

DOI: 10.1134/S1064226918080090

INTRODUCTION

During the past decade, the interest of the scientific community to the so-called metamaterials and metastructures, which possess specific electromagnetic properties not inherent in natural materials, has not diminished. Metamaterials, among others, include a large group of volume or surface structures that have frequency intervals in which the propagation of electromagnetic waves is impossible. Structures of this group are usually referred to as PBG (photonic band gap) or EBG (electromagnetic band gap) structures. Among the problems solved with the help of EBG structures, a special place belongs to the problem of suppressing parasitic surface waves in antenna devices and complex microwave circuits. To suppress surface waves, a number of authors proposed structures with a high surface impedance [1–14]. In particular, in article [1], which was published in 1999 and now became classical, a high-surface-impedance structure consisting of a periodic array of electrically conducting mushroom-shaped elements on an electrically conducting screen was described. This structure is also an artificial magnetic conductor, because, under the incidence of a plane electromagnetic wave, an electric antinode and a magnetic node on its surface form. These properties in the operating frequency band are due to the parallel resonance in elementary *LC*-resonators, each of which is formed by two neighboring mushroom elements and the corresponding part of the surface of the electrically conducting screen. The "mushroom caps" in specific examples had a square and hexagonal shape. In [1], the advantages of using such a structure as a "ground plane" of antenna systems was noted.

Almost simultaneously with [1] and in subsequent years, a number of works appeared in which new structures and applications of high-impedance surfaces were described. These structures usually included a capacitive array made of electrically conducting elements of various shapes, an electrically conducting screen, and short conductors connecting each element of the array to the screen [1–7]. The search for optimal shapes of arrays elements was aimed, in particular, at reducing the frequency, expanding the working range, and increasing the angular stability of the devices proposed. In some cases, the developers abandoned the use of conductors connecting the array elements to the screen [8–13].

A special place among the works published to date belongs to [14], where the structure of an artificial magnetic conductor (high-impedance surface) without an electrically conducting screen was proposed. This design comprises a three-dimensional block of metamaterial based on C-shaped metal elements the planes of which are oriented perpendicularly to the magnetic field of the incident wave. The working frequencies of such an artificial magnetic conductor are rather high and amount to 10 ± 0.5 GHz. One of the

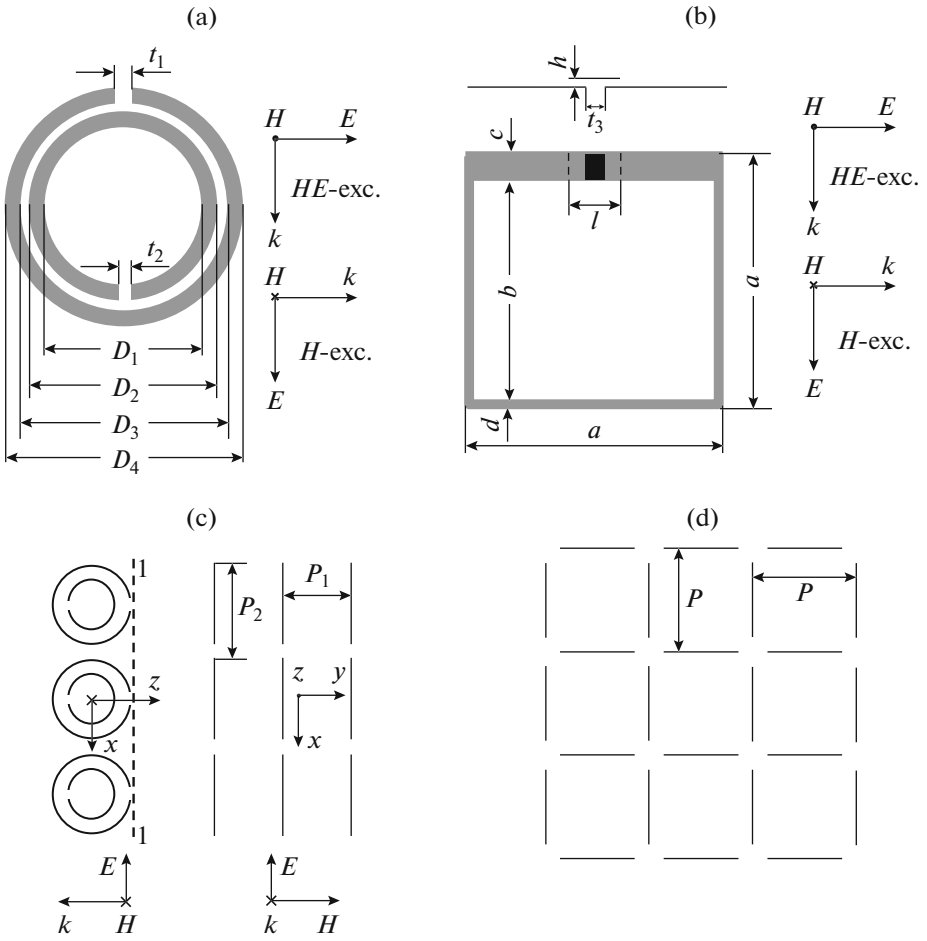

Fig. 1. Elements of periodic arrays and arrays of these elements: (a) a double split-ring resonator, (b) a single square split-ring resonator with a capacitive shunt, (c) an array for one polarization, and (d) an array for two polarizations.

ways to increase the working wavelength of this device would be a proportional change in the dimensions of the C-element. Another way is to change the shape of the element in order to increase its capacitance or inductance. An example of such an element can be a double split-ring resonator, used in metamaterials with negative permittivity and permeability [15, 16].

In this paper, we consider an artificial magnetic conductor (high-impedance surface), which comprises an array of double split-ring resonators, or an array of single split-ring resonators with capacitive shunts across the gaps. Such a single-layer structure of an artificial magnetic conductor also does not require the presence of an electrically conducting screen.

1. REFLECTION COEFFICIENTS OF PERIODIC ARRAYS OF DOUBLE AND SINGLE SPLIT-RING RESONATORS

Figure 1 shows the elements of periodic arrays: a double split-ring resonator (Fig. 1a) and a single split-ring resonator with a capacitive shunt across the gap in the conductor (Fig. 1b), and also an array of such elements (Figs. 1c and 1d). The capacitive shunt is made in the form of a metal strip of length l and a gap of width h between the strip and the ring, as shown in Fig. 1b. The planes of the rings in the arrays are parallel to the direction of the wave propagation.

Figure 2 shows the calculated frequency dependences of the amplitude and phase of the reflection coefficients of the incident electromagnetic wave for arrays of double-split ring resonators (Fig. 2a) and single split-ring resonators with a capacitive shunt (Fig. 2b) in the region of the low-frequency resonance of the circular current. The dimensions of the rings are $D_1 = 3.0$ mm, $D_2 = 4.6$ mm, $D_3 = 5.0$ mm, $D_4 = 6.6$ mm, $t_1 = 0.3$ mm, $t_2 = 0.2$ mm, $a = 5$ mm, $b = 4.3$ mm, $c = 0.5$ mm, $d = 0.2$ mm, $l = 1.08$ mm, $h = 0.05$ mm, and $t_3 = 0.3$ mm; the periods of the arrays are $P_1 = P_2 = 10$ mm; and the relative permittivities of the substrates of metal elements are set in the calculations to unity. Hereinafter, the calculations were carried out using the FEKO program.

The frequency dependences in Figs. 2a and 2b were calculated for two orientations of the rings with respect to the electromagnetic field of the incident wave, corresponding to the magnetic (*H*) and magnetoelectric (*HE*) excitation of the circular currents in the array of rings (see Figs. 1a and 1b) (hereinafter, we use the terms *H*- and *HE*-excitation, as well as *H*- and *HE*-orientation of the rings). It follows from Figs. 2a and 2b that the resonance frequencies of the arrays with the *HE*-orientation of the rings are slightly smaller than those for the *H*-orientation. At these frequencies, the phases of the reflection coefficients for the *H*-orientation are close to zero and, for the *HE*-orientation, are 60° and 90° for arrays of double and single split-ring resonators, respectively. The phase of the reflection coefficient is measured from the plane passing through the geometric centers of the array elements. In this case, the phase of the reflection coefficient for transverse planes in front of the array will be smaller by $(720z/\lambda)°$, where z is the distance from the center of the ring to the plane from which the phase is measured and λ is the wavelength at which the phase is determined. We see that, for the *H*-orientation of the rings, the phase of the reflection coefficient at the resonance in front of the array is negative and, for the *HE*-orientation, there can be planes in front of the array on which these phases are zero, i.e., the arrays have the properties of an artificial magnetic conductor or a high-impedance surface. At the resonance frequency, the coordinate $z_{01,2}$, corresponding to the zero phase of the reflection coefficient, can be determined from the following equations: for a double split-ring resonator,

$$60 - (720z_{01}/\lambda_{01}) = 0, \quad (1)$$

and, for a single split-ring resonator,

$$90 - (720z_{01}/\lambda_{02}) = 0, \quad (2)$$

where $\lambda_{01} = 4.66$ cm and $\lambda_{02} = 4.96$ cm are the resonance wavelengths of the arrays of double and single split-ring resonators, respectively. It follows from Eqs. (1) and (2) that $z_{01} = 3.9$ mm and $z_{02} = 6.2$ mm.

It should be noted that the zero phase of the reflection coefficient is not a sufficient condition for the implementation of an artificial magnetic conductor or a high-impedance surface, since the reflection coefficient is determined in a plane remote from the surface of the array, where local non-propagating waves are already absent. Near the array, the electromagnetic field is very nonuniform and the impedance in this region must be determined using the averaged values of the electric and magnetic fields.

2. THE ELECTRIC AND MAGNETIC FIELDS NEAR THE ARRAY

Figures 3a and 3b show the calculated distribution of the transverse field components E_x (solid lines) and

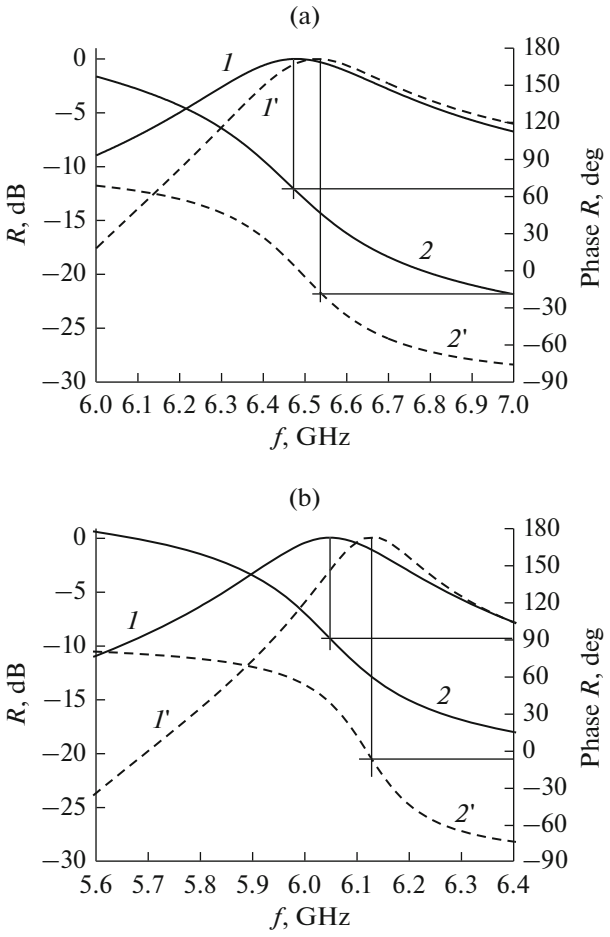

Fig. 2. Frequency dependences of the reflection coefficients for the cases of (solid curves) *H*-excitation and (dashed curves): *HE*-excitations: (*1*, *1'*) absolute values and (*2*, *2'*) phase of the reflection coefficients of arrays of (a) double split-ring resonators and (b) single split-ring resonators with a capacitive shunt.

H_y (dashed lines) along the z-coordinate, perpendicular to the plane of the array at a resonance frequency for several values of x and y for the *H*- and *HE*-orientations of a double split-ring, respectively. The vertical lines in these figures at $z = 3.3$ mm indicate the boundaries of the arrays. The cross section $z = 0$ passes through the geometric centers of the array elements. A comparative analysis of the data presented in Figs. 3a (*H*-excitation) and 3b (*HE*-excitation) allows us to make some remarks about the structure of the electromagnetic field near and inside the array. In particular, in the case of the *H*-excitation of array elements, the maxima of E_x lie in the interval $z = 1.5...3.5$ mm and the minima of H_y lie in the interval $z = 2.2...5$ mm; for $y = 0$ and $x = 5$ mm, this minimum is large, i.e., differs little from the neighboring maximum. Under the *HE*-excitation, the maxima of E_x lie in the interval $z = 4...6$ mm and the minima

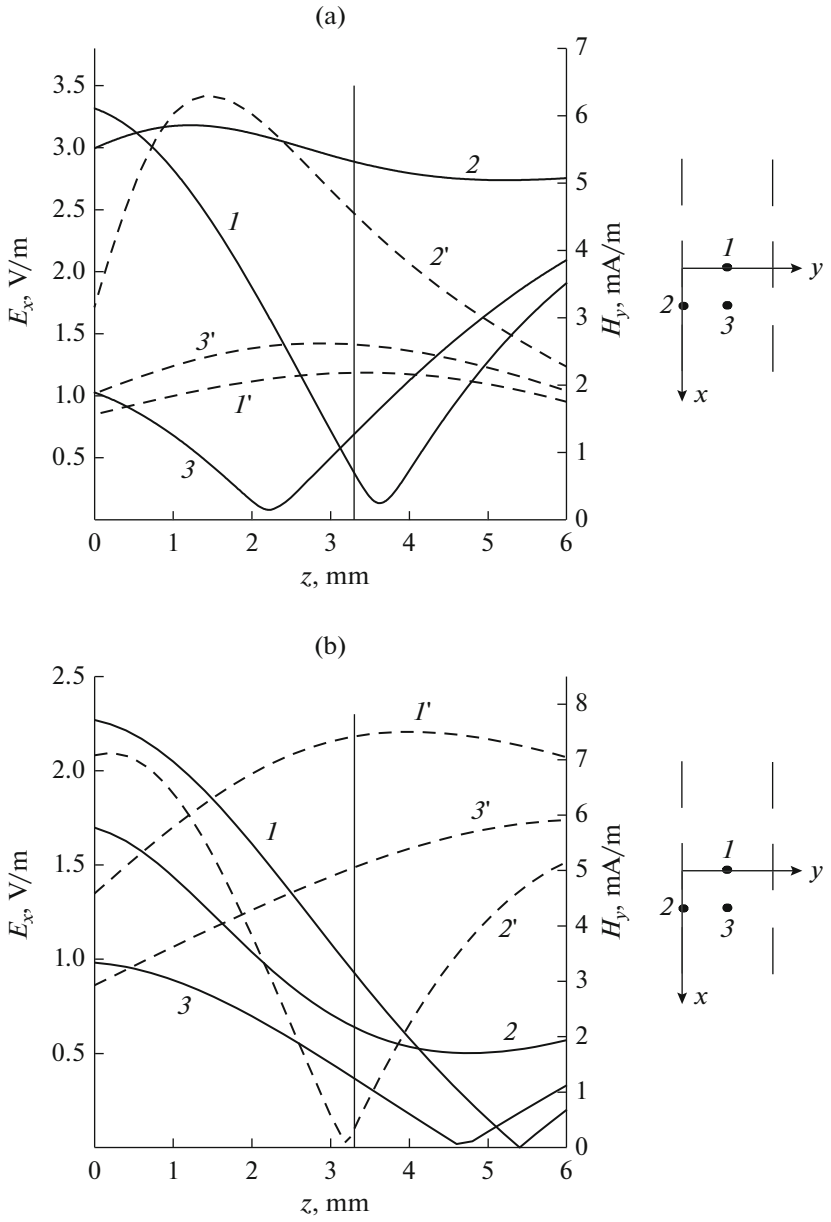

Fig. 3. Electromagnetic field distribution the near the arrays. Dependences (solid curves) $H_y(z)$ and (dashed curves) $E_x(z)$ for the case of (a) *H*-excitation and (b) *HE*-excitation of an array of double split-ring resonators for (*1*, *1*') $x = 0$, $y = 5$ mm, (*2*, *2*') $x = 5$ mm, $y = 0$; and (*3*, *3*') $x = y = 5$ mm.

of H_y are relatively deep and lie in a narrow interval $z = 4.5$–5.5 mm.

As expected, the electromagnetic field near the array is nonuniform and, therefore, the impedance $|Z|$ in the plane xy should be defined as the ratio of the x, y-averaged electric and magnetic fields.

Figure 4a shows the impedances $|Z|$ as a function of the z-coordinate for the *H*- (curve *1*) and *HE*-excitation (curves *2* and *3*). As expected, the impedances of the arrays of double split-ring resonators under the *H*-excitation proved to be many times smaller than the impedances under the *HE*-excitation. The maxima of the impedance under the *HE*-excitation are located at a distance of about 1.5 mm from the boundary of the array and amount to several thousand ohms. Figure 4b shows similar calculated dependences for arrays of single split-ring resonators with a capacitive shunt under the *H*- (curve *1*) and *HE*-excitation (curves *2*–*5*).

In the calculations, two types of shunts were used: a short shunt (curves *1*–*4*) with the same dimensions as in calculating the reflection coefficient in Fig. 2b ($l = 1.08$ mm, $h = 0.05$ mm) and a long shunt with the

dimensions $l = 5$ mm and $h = 0.25$ mm (curve *5*). In this case, the resonance frequencies f_0 of the arrays, represented by curves *4* and *5*, were the same and equal to 5.55 GHz.

As in the case of an array of double split-ring resonators, the impedances under the *H*-excitation of single split-ring resonators turned out to be small in comparison with the impedances under the *HE*-excitation. In this case, the maxima of the impedances under the *HE*-excitation amount to 20000 Ω but are located slightly further from the boundary of the array than in the case of double split-ring resonators. The maximum of the impedance in the case of rings with a short capacitive shunt is substantially farther from the plane of the array than in the case of a long shunt.

The high-impedance effect can be demonstrated on a Salisbury radio-absorbing structure.

3. MODIFIED SALISBURY RADIO-ABSORBER

As is known, a Salisbury radio-absorber is a quarter-wave dielectric layer one side of which is metallized and the other side is covered by a resistive film with a specific impedance of 120π Ω per square. The total energy absorption in such a film is due to the fact that it is located at the maximum of the electric field and the minimum of the magnetic field, i.e., in the plane of a high-impedance. It is natural to expect a similar absorption effect from placing such a resistive film near an array of double or single split-ring resonators under the *HE*-excitation of the array elements.

Figure 5a shows the calculated dependences of the reflection and transmission coefficients for an array of double split-ring resonators with a resistive film placed in the plane $z = 4.6$ mm; i.e., at a distance of 1.3 mm from the boundary of the array. For comparison, in the same graph, the frequency dependences of the reflection and transmission coefficients for the same array in the absence of a resistive film are given.

The absorption effect was confirmed experimentally by a waveguide method on an array of 24 double split-ring resonators and a resistive film with a specific impedance of 500 Ω per square. The array elements were placed into a matrix of foamed polystyrene enclosed in a waveguide with a 48×24 mm^2 cross section (see the inset on the right in Fig. 5b). The same figure shows the measured frequency dependences of the reflection and transmission coefficients for an array with a resistive film placed at a distance of 1 mm from the array and in the absence of a resistive film.

Thus, the calculations have shown and the measurements have confirmed the presence of a high impedance near the surface of an array of *HE*-excited split-ring elements. This fact makes it possible to use such arrays as reflective screens for low-profile antennas.

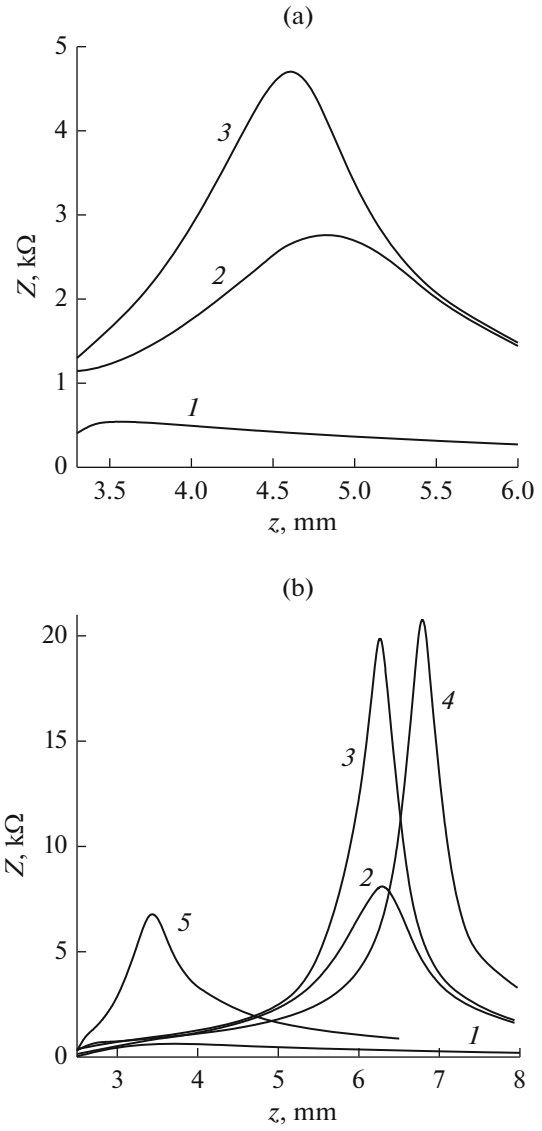

Fig. 4. Impedance distribution near the arrays: (a) dependence $Z(z)$ for an array of double split-ring resonators in the case of (*1*) *H*-excitation and $P_1 = P_2 = 10$ mm; (*2*) *HE*-excitation, $P_1 = P_2 = 10$ mm, and (*3*) $P_1 = P_2 = 7$ mm; (b) dependence $Z(z)$ for an array of single split-ring resonators with a capacitive shunt (*1*) under the *H*-excitation and $P_1 = P_2 = 10$ mm, $l = 1.08$ mm, and $h = 0.05$ mm and (*2*) under the *HE*-excitation and $P_1 = P_2 = 10$ mm, $l = 1.08$ mm, and $h = 0.05$ mm; (*3*) $P_1 = P_2 = 7$ mm, $l = 1.08$ mm, and $h = 0.05$ mm; (*4*) $P_1 = 2.5$ mm, $P_2 = 5.5$ mm, $l = 1.08$ mm, and $h = 0.05$ mm, and (*5*) $P_1 = 2.5$ mm, $P_2 = 5.5$ mm, $l = 5$ mm, $h = 0.25$ mm.

4. A FINITE ARRAY OF IDENTICAL SINGLE SPLIT-RING RESONATORS AS A SCREEN FOR A DIPOLE ANTENNA

Consider a dipole with a diameter of 1 mm and length L, located at a distance of $\delta = 2$ mm from an array of open single-split ring resonators with capaci-

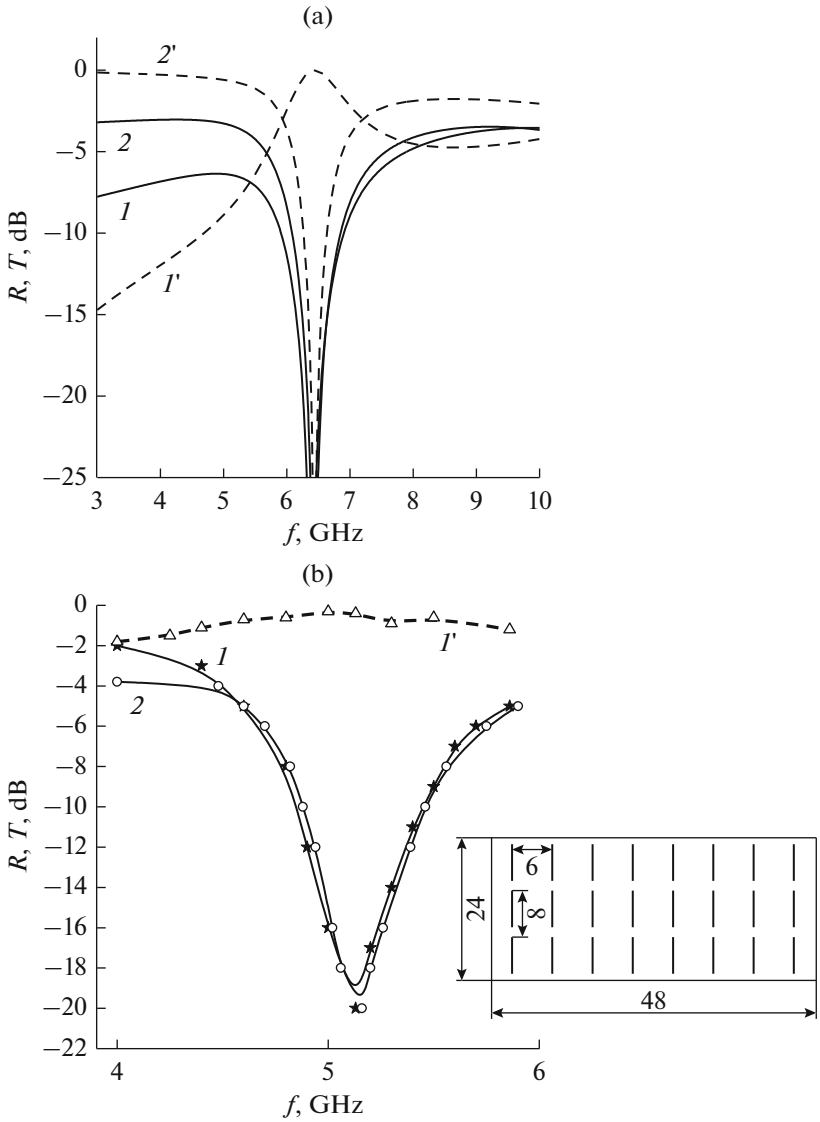

Fig. 5. (a) Calculated and (b) measured frequency dependences of (*1*, *1*') the reflection coefficients and (*2*, *2*') propagation constants in the presence or in the absence of a resistive film near the surface of the array: (a) calculation for arrays of double split-ring resonators with a period of $P_1 = P_2 = 7$ mm under the *HE*-excitation (solid curves) with a resistive film having a specific impedance of 120 Ω per square and (dashed curves) without a resistive film; (b) experiment for an array of 24 double split-ring resonators (solid curves) with a resistive film having a specific impedance of 500 Ω per square and (dashed curves) without a resistive film.

tive shunts with the sizes $l = 5$ mm and $h = 0.25$ mm (Fig. 6a). The periods of the array are $P_1 = 2.5$ mm and $P_2 = 5.5$ mm, and the number of elements is 48 (6 × 8). The calculated resonance frequency of an infinite array was $f_0 = 5.55$ GHz, and the wavelength was $\lambda_0 = 54$ mm. The radiation patterns $F(\vartheta)$ in the sector of angles from −180° to 180° (the angles ϑ in the *E*- and *H*-planes are measured from the normal to the array on the side of the incidence), and the reflection coefficient S_{11} of the line feeding the dipole in the frequency range of 4–6 GHz for several lengths of the dipole were calculated. The wave impedance of the feed line is 50 Ω. The calculation results are given in Table 1.

The resonance frequency of a structure of limited size f_{res}, which was determined from the minimum $F(180°)$ and the maximum $F(0°)$, proved to be slightly lower then f_0 and depended on the length of the dipole weakly. The values of $F(0°)/F(180°)$ and S_{11} are given at the resonance frequencies. Table 1 also presents the matching frequencies f_{match}, at which the dipole is matched best to the feed line. As follows from the data of Table 1, as the dipole is made shorter, the frequencies f_{match}, being initially lower than the resonance fre-

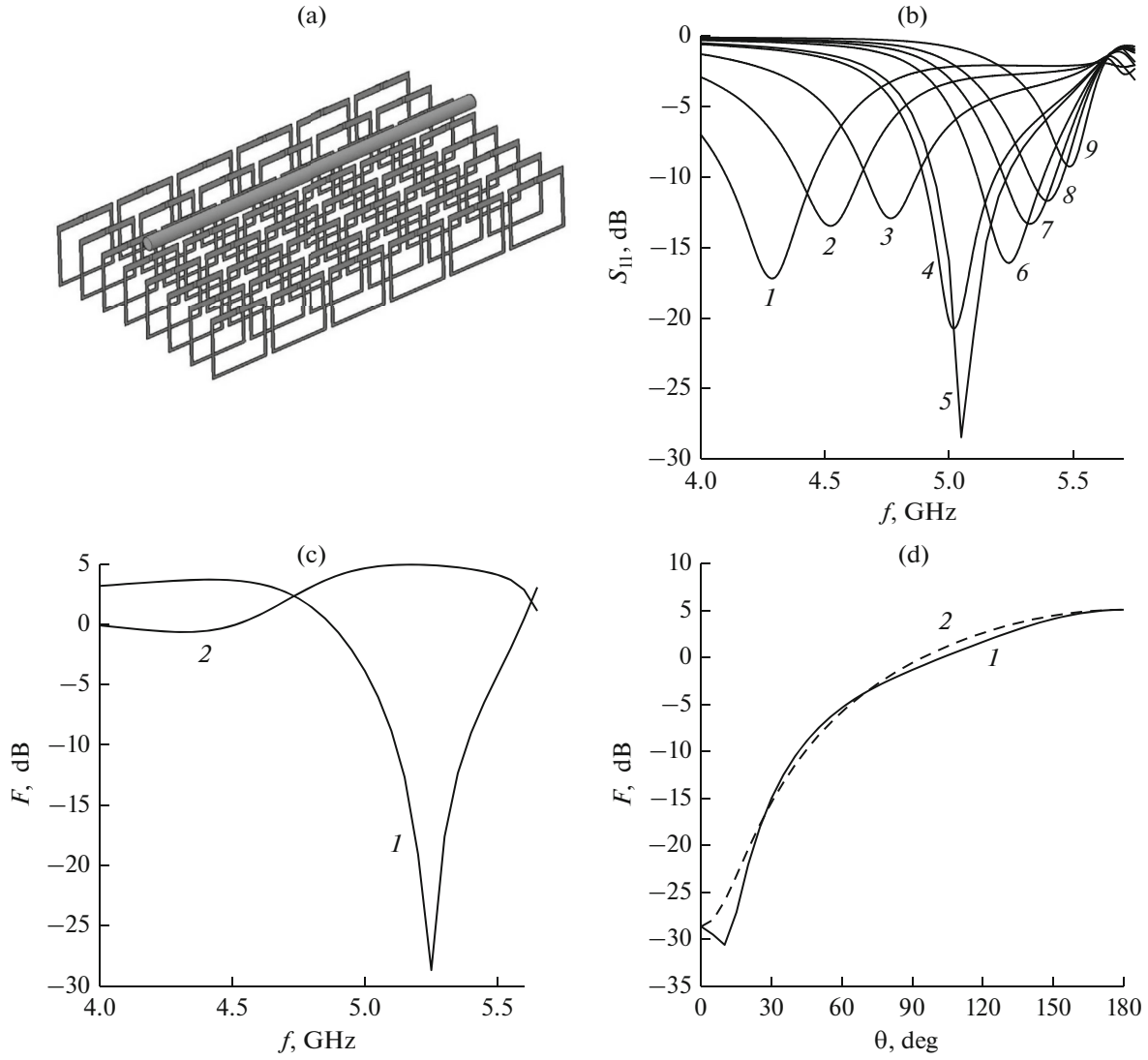

Fig. 6. Matching and radiation characteristics of a capacitive dipole near an array of identical single split-ring resonators with a capacitive dipole: (a) an array with a dipole, (b) frequency dependences of the reflection coefficient S_{11} in a line feeding the dipole for nine values of the dipole length: (*1*) 30, (*2*) 27.5, (*3*) 25, (*4*) 22.5, (*5*) 22, (*6*) 20, (*7*) 19, (*8*) 18, and (*9*) 16 mm; (c) frequency dependences of the amplitude radiation pattern at a resonant frequency for the angles (*1*) $\vartheta = 0°$ and (*2*) 180° for a dipole of length $L = 20$ mm; (d) angular dependences of the amplitude radiation pattern $F(\vartheta)$ at a resonance frequency $f_{res} = 5.25$ GHz for a dipole of length $L = 20$ mm in the (*1*) *E*- and (*2*) *H*-planes.

quencies, approach these frequencies, reach them, and then exceed them. At $f_{res} = f_{match}$, the reflection coefficient S_{11} is minimal; i.e., the conditions for matching the dipole to the feed line are optimal.

It should be noted that, at the aforementioned periods P_1 and P_2 of the array and parameters l and h of the capacitive shunt, the emitting dipole is located near the maximum of the impedance Z, i.e., as if on the surface of an artificial magnetic conductor (see Fig. 4b, curve *5*). As noted in [4], this arrangement of the dipole is not optimal in terms of the matching to the feed line. Therefore, it is necessary to shift the maximum of Z with respect to the location of the dipole, which can be implemented by using a capacitive shunt of small length l (see Fig. 4b, curve *4*). The radiation pattern $F(\vartheta)$ and the reflection coefficient S_{11} of a radiating dipole over an array of single split-ring resonators with short capacitive shunts ($l = 1.08$ mm, $h = 0.05$ mm) were calculated. With these parameters of the shunt, the resonance values of f_0 and λ_0 for an infinite array remain approximately the same as in the previously considered case. The calculation results are given in Table 2.

Figure 6b shows the frequency dependences of the reflection coefficient S_{11} for several dipole lengths in

Table 1. Characteristics of radiation and matching of a dipole near an array of single split-ring resonators with long capacitive shunts for $P_1 = 2.5$ mm, $P_2 = 5.5$ mm, $\delta = 2$ mm, $l = 5$ mm, and $h = 0.25$ mm

L, mm	L/λ	f_{res}, GHz	$F(0°)/F(180°)$, dB	S_{11}, dB	f_{match}, GHz
30	0.55	5.25	35	−2	4.27
27.5	0.51	5.2	33	−3	4.52
25	0.46	5.2	35	−4	4.72
22.5	0.42	5.18	27	−6	4.93
20	0.37	5.15	28	−11	5.08
19	0.35	5.15	28	−10	5.17
18	0.33	5.15	28	−7	5.23

Table 2. Characteristics of radiation and matching of a dipole near an array of single split-ring resonators with short capacitive shunts for $P_1 = 2.5$ mm, $P_2 = 5.5$ mm, $\delta = 2$ mm, $l = 1.08$ mm, and $h = 0.05$ mm

L, mm	L/λ	f_{res}, GHz	$F(0°)/F(180°)$, dB	S_{11}, dB	f_{match}, GHz
30	0.55	5.32	24	−2	4.28
27.5	0.51	5.31	27	−3	4.53
25	0.46	5.28	27	−4	4.77
22.5	0.42	5.25	32	−8	5.03
22	0.41	5.25	33	−10	5.06
20	0.37	5.25	33	−16	5.23
19	0.35	5.25	32	−12	5.33
18	0.33	5.25	31	−7	5.40
16	0.30	5.24	29	−2.5	5.49

the interval 16–30 mm. For example, Fig. 6c shows the frequency dependences of $F(0°)$ and $F(180°)$ for a dipole of length $L = 20$ mm, and Fig. 6d shows the angular dependences of the amplitude of the radiation pattern $F(\vartheta)$ at the resonance frequency $f_{res} = 5.25$ GHz.

As follows from the comparison of the data given in Tables 1 and 2, the arrays of split-ring resonators with short capacitive shunts provide better matching of the dipole to the feed line at the resonant frequencies of the array, f_{res}. In particular, the reflection coefficient S_{11} in the feed line at the frequency f_{res} does not exceed −10 dB for dipoles of lengths 19–22 mm, and the frequency f_{res} changes little as the dipole length varies in the interval 16–30 mm.

Table 3 given the values of f_{res}, f_{match}, $F(0°)/F(180°)$, and S_{11} for a dipole of length $l = 20$ mm and four distances δ between the dipole and the array. It can be seen that, with decreasing distance δ, the frequency f_{res} is almost invariable, and the frequency f_{match} slightly decreases. The reflection coefficient in the line noticeably increases. It is easy to see that, by adjusting within a small range the dipole length for different δ so that $f_{res} = f_{match}$ it is possible to ensure the best matching of the dipole to the feed line. Table 4 presents the corresponding values of δ, L, $f_{res} = f_{match}$, $F(0°)/F(180°)$, and S_{11}.

Thus, the data presented in Fig. 6 and Tables 1–4 allow us to conclude that, for any radiation frequency, it

Table 3. Characteristics of radiation and matching of a dipole of length $L = 20$ mm near an array of single split-ring resonators with short capacitive shunts for different δ

δ, mm	f_{res}, GHz	f_{match}, GHz	$F(0°)/F(180°)$, dB	S_{11}, dB
2.0	5.25	5.24	33	−16
1.5	5.23	5.17	29	−15
1.0	5.20	5.10	31	−12
0.5	5.20	5.03	30	−7

Table 4. Characteristics of radiation and matching of an optimal-length dipole for different δ

δ, mm	l, mm	$f_{res} = f_{match}$, GHz	$F(0°)/F(180°)$, dB	S_{11}, dB
2.0	20	5.25	33	−16
1.5	19.3	5.23	29	−20
1.0	18.8	5.20	31	−25
0.5	18	5.20	26	−15

is possible to determine the period and dimensions of the array elements, as well as the length of the dipole and its distance to the array, that afford the best matching of the dipole with the supply line ($S_{11} < -20$ dB) and sufficiently large (more than 30 dB) ratio between the amplitudes of the reflected and transmitted fields, $F(0°)/F(180°)$.

CONCLUSIONS

It has been shown that, for the *HE*-orientation of elements of an array of double split-ring resonators or single split-ring resonators with a capacitive shunt, in close vicinity of the array, there are planes in which the phase of the reflection coefficient is zero; i.e., the array possesses the properties of an artificial magnetic conductor or a high-impedance surface.

At the resonance frequencies, in the planes parallel to the array, the impedances determined by the ratio of the electric and magnetic fields averaged over the plane near the arrays have been calculated. In this case, the maximum impedance under the *HE*-excitation of the array elements were 4700 Ω for arrays of double split-ring resonators and 21000 Ω for arrays of single split-ring resonators with a capacitive shunt. The presence of a high impedance in the planes close to the array has been confirmed theoretically and experimentally by the strong absorption of the energy of an incident wave when a resistive film with a specific impedance close to the wave impedance of free space was placed near the array.

The calculation of the radiation pattern of a dipole near a finite array of single split-ring resonators with capacitive shunts have shown the possibility of using such an array as a reflecting screen for low-profile antennas. In this case, the screening effect (the ratio of the amplitudes of the reflected and transmitted fields) can exceed 30 dB with a good matching of the dipole to the feed line (the reflection coefficient in the line is less than −20 dB).

REFERENCES

1. D. Sievenpiper, L. Zhang, R. F. J. Broas, et al., IEEE Trans. Microwave Theory Tech. **47**, 2059 (1999).
2. R. F. J. Broas, D. F. Sievenpiper, and E. Yablonovitch, IEEE Trans. Microwave Theory Tech. **49**, 1262 (2001).
3. S. Clavijo, R. E. Díaz, and W. E. McKinzie, IEEE Trans. Antennas Propag. **51**, 2678 (2001).
4. F. Yang and Y. Rahmat-Samii, IEEE Trans. Microwave Theory Tech. **51**, 2691 (2003).
5. C. R. Simovski, P. de Maagt, S. A. Tretyakov, et al., Electron. Lett. **40** (2), 92 (2004).
6. R. F. J. Broas, D. F. Sievenpiper, and E. Yablonovitch, IEEE Trans. Microwave Theory Tech. **53**, 1377 (2005).
7. N. Kushwaha and R. Kumar, J. Microw. Optoelectron. Electromagn. Appl. **13** (1), 16 (2014).
8. F.-R. Yung, K.-P. Ma, and Y. Qian, IEEE Trans. Microwave Theory Tech. **47**, 2092 (1999).
9. R. Coccioli, F.-R. Yung, K.-P. Ma, and T. Itoh, IEEE Trans. Microwave Theory Tech. **47**, 2123 (1999).
10. Y. Zhang, J. von Hagen, M. Younis, et al., IEEE Trans. Microwave Theory Tech. **51**, 2704 (2003).
11. A. P. Feresidis, G. Goussetis, Sh. Wang, and J. C. Vardaxoglou, IEEE Trans. Microwave Theory Tech. **53**, 209 (2005).
12. D. J. Kern, D. H. Werner, A. Monorchio, et al., IEEE Trans. Microwave Theory Tech. **53**, 8 (2005).
13. Yu. N. Kazantsev and V. N. Apletalin, J. Commun. Technol. Electron. **52**, 390 (2007).
14. M. A. Hiranandani, A. B. Yakovlev, and A. A. Kishk, IEE Proc. Microw. Antennas Propag. **153**, 487 (2006).
15. M. V. Kostin and V. V. Shevchenko, in *Proc. 3rd Int. Workshop on Chiral, Bi-Isotropic and Bi-Anisotropic Media, (CHIRAL'94), Perigueux, France, 1994*, p. 49.
16. J. B. Pendry, A. J. Holden, D. J. Robbins, and W. J. Stewart, IEEE Trans. Microwave Theory Tech. **47**, 2075 (1999).

Translated by E. Chernokozhin